ACS APPLIED MATERIALS & INTERFACES

Research Article

www.acsami.org

Construction of Degradable Multilayer Films for Enhanced Antibacterial Properties

Bai-liang Wang, Ke-feng Ren,* Hao Chang, Jin-lei Wang, and Jian Ji*

MOE Key Laboratory of Macromolecule Synthesis and Functionalization, Department of Polymer Science and Engineering, Zhejiang University, Hangzhou 310027, China

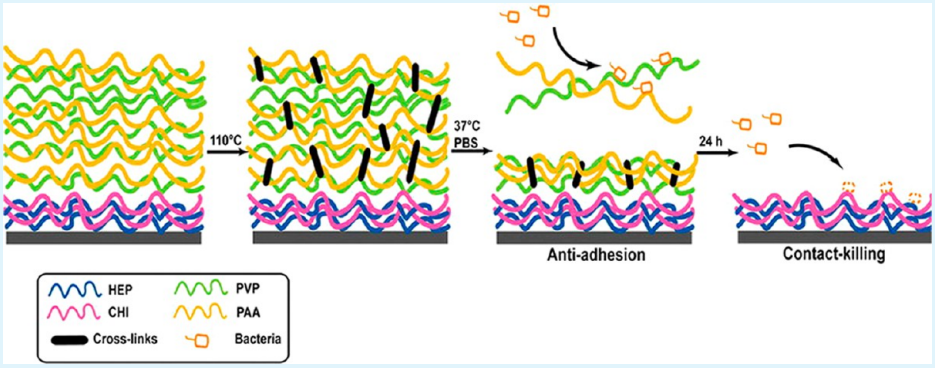

ABSTRACT: Infections associated with medical devices have become a major concern. The adhesion of bacteria to the devices' surfaces during the initial 24 h is believed to be a "decisive period" for implant-associated infections, which pose key challenges to optimal antiadhesion of microbes in this period. Herein, we have designed and constructed a $(\text{heparin/chitosan})_{10}$–$(\text{polyvinylpyrrolidone/poly(acrylic acid)})_{10}$ $[(\text{HEP/CHI})_{10}$–$(\text{PVP/PAA})_{10}]$ multilayer film by layer-by-layer self-assembly. Assembly of the underlying $(\text{HEP/CHI})_{10}$ multilayer film is based on electrostatic interactions, showing the properties of contact killing of bacteria. Deposition of the top $(\text{PVP/PAA})_{10}$ multilayer film is based on hydrogen bond interactions. The PAA molecules are then cross-linked to form anhydride groups by thermal treatment at 110 °C for 16 h. Therefore, it shows a top-down degradable capability in the determined period, leading to almost no adhesion of bacteria in 24 h. Our system combining the adhesion resistance and the contact killing properties shows an enhanced antibacterial capability through targeting the "decisive period" of implantation may have great potential for applications in medical implants, tissue engineering, etc.

KEYWORDS: *antibacterial, degradable, implant-associated infections, layer-by-layer self-assembly, thermal cross-linking, poly(acrylic acid)*

1. INTRODUCTION

Microbial infection is one of the most serious problems in the field of medical devices, particularly in implants.[1,2] Approximately more than half of all nosocomial infections are attributed to implant-associated infections, leading to the death of at least one million persons in the US per year.[2,3] Even worse, the extraction of contaminated implants is generally the only option for eliminating infections due to the lack of suitable treatment.[3]

The adhesion of bacteria on the surface of implants is the first and key step for late formation of bacterial colonization and the biofilm, which is a big threat to the long-term success of the implants.[4] How to design and construct a surface for controlling bacterial adhesion has therefore become a research hotspot. The adhesion of bacteria is a very complicated process, and it basically includes two stages:[5] (I) an initial, rapid, and reversible interaction; (II) a slowly irreversible adhesion through specific and nonspecific interactions. Consequently, three main strategies have been developed.[5] The first one is a surface with "adhesion resistance" properties. Polymers such as poly(ethylene glycol) (PEG),[6,7] poly(ethylene oxide) (PEO) brushes,[8] and polyvinylpyrrolidone (PVP)[9,10] are used to modify materials for creating superhydrophilic and nonfouling surfaces.[11] Recently, the superhydrophobic surfaces have also been studied for resisting bacterial adhesion.[12,13] However, the effectiveness of these adhesion resistant surfaces could be decreased and even totally lost because of instability of molecules or contamination by the conditioning substances under the physiological environment.[14] The second strategy is a "contact-killing" surface, where the surfaces are capable of killing bacteria through direct contact. The surfaces could be prepared by grafting,[15] covalent linking,[16,17] or self-assembly[18] of antimicrobial compounds, among which quaternary ammonium compounds[19] have been widely investigated. A major problem with this kind of surface is the covering of dead bacteria's bodies, which could significantly reduce the efficiency

Received: January 7, 2013
Accepted: April 19, 2013
Published: April 19, 2013

   dx.doi.org/10.1021/am4000547 | ACS Appl. Mater. Interfaces 2013, 5, 4136–4143

of the contact-killing. And it could even trigger immune response and inflammation.[20] The third strategy is a "biocide leaching" surface. Coatings that actively release antibacterial agents, such as antibiotics[21,22] and silver ions,[23,24] can reduce bacterial adhesion and eradicate infection. However, the growing number of bacteria that show resistance to antibiotics and the side-effects of antibiotics on mammal cells or tissues are the main limitations.[25] Many efforts have been made to combine these two or even three strategies together for higher antibacterial efficiency. For instance, Jiang and co-workers have reported a switchable polymer system, which shows antimicrobial ability due to cationic molecules. More importantly, the dead bacteria can be released when the cationic derivatives are hydrolyzed to nonfouling zwitterionic polymers.[20,26] However, the continuous attack and contamination by the proteins and microbes in in vivo conditions could limit its long-term application.

The first 24 h after an implantation of a biomedical device has been considered as a "decisive period", during which microbes can easily adhere and colonize on implants.[14] The reason could be the compromised immune system of patients whose defensive cells show weak bactericidal activities. Prevention of microbes' adhesion during this decisive period is critical and can thus significantly increase the long-term success rate of biomedical implants.[2,27] Unfortunately, there are rarely reports addressing this issue. Ideally, we envision that a dynamic surface with continuous degradation should maximally inhibit bacteria adhesion. In theory, the controlling cross-linking density of a degradable system could be a good way to create such a dynamic surface. For instance, Rubner et al. have reported a (PAA/polyacrylamide) multilayer film based on layer-by-layer (LbL) self-assembly. The film can be thermally cross-linked, and it would resist deconstruction in a controllable period through regulating the cross-linking degree.[28]

Previously, we have demonstrated a (heparin/chitosan) (HEP/CHI) multilayer film, showing both reduced bacterial adhesion and the ability to kill adhered bacteria.[18] In the present study, we have further developed it through constructing a top-down degradable film onto the (HEP/CHI) multilayer film for enhanced antibacterial properties. A multilayer film of (PVP/poly(acrylic acid) (PAA)) based on hydrogen bond interactions is employed to serve as a top-down degradable part. The (PVP/PAA) multilayer film is treated by thermal cross-linking to control the degradation rate. A top-down degradable film, where the time of degradation is precisely controlled over 24 h, shows significant advantages, since continuous removal of the outmost surface totally inhibits bacterial adhesion. Furthermore, after removal of the (PVP/PAA) film, the underlying (HEP/CHI) multilayer film will be exposed and provide contact-killing antibacterial properties for systemic bacteria circulating in the body.[29] We chose PVP and PAA as the components for the degradable multilayer film for the following reasons: (1) there are hydrogen bond interactions between PAA and PVP; (2) PAA can be cross-linked by thermal treatment to form a degradable anhydride group; (3) both PAA and PVP have good biocompatibility.[30−32] Although not all biomedical devices can be thermally treated at high temperature, our multilayer film could be potentially applied to biomedical devices made by some polymers and metal, such as steel stents and bone nails. Data of ellipsometry and quartz crystal microbalance (QCM) confirm the successful construction of the $(HEP/CHI)_{10}$−$(PVP/PAA)_{10}$ multilayer film. We found that, after thermal treatment at 110 °C for 16 h, the degradation time of the top (PVP/PAA) film can be controlled over 24 h, leading to almost no bacterial adhesion during the experiments. After 24 h degradation, the underlying (HEP/CHI) film is exposed, showing contact-killing properties, as confirmed by a LIVE/DEAD bacterial viability kit.

2. EXPERIMENTAL SECTION

2.1. Materials. CHI (M_w: 410 kDa, 91% deacetylation) was obtained from Qingdao Haihui Corporation of China. PVP (K value: 29−32), poly(ethyleneimine) (branched PEI, M_w: 25 kDa), and PAA (M_w: 10 kDa) were purchased from Sigma-Aldrich. HEP (sodium salt) was obtained from Shanghai Chemical Reagent Company of China. Trypticase soy agar (TSA) and trypticase soy broth (TSB) were purchased from Hangzhou Baisi Corporation of China. *Staphylococcus aureus* (*S. aureus*, ATCC 6538) was kindly provided by Prof. Jian Xu (Zhejiang Chinese Medical University, Hangzhou, China). Ultrapure distilled water was used from a Millipore Milli-Q system (USA).

2.2. Construction and Degradation of the $(HEP/CHI)_{10}$−$(PVP/PAA)_{10}$ Multilayer Film. Silicon wafers and glass slides were used as substrates and cleaned by Piranha solution (H_2SO_4/H_2O_2 = 7:3) (*Caution: Piranha solution can react violently with many organic materials and should be handled extremely carefully!*).[33] Substrates were first immersed into PEI solution (5 mg/mL) for 30 min to form a precursor layer. For the underlying $(HEP/CHI)_{10}$ multilayer film, the substrates were alternately dipped in HEP and CHI solution (1 mg/mL in HAc/NaAc buffer, 0.1 M at pH 4.0) for 10 min and subsequently rinsed with HAc/NaAc buffer. After that, the samples were then ready for deposition of the top $(PVP/PAA)_{10}$ multilayer film. PVP and PAA were dissolved in pure water at 1 mg/mL at predetermined pH value. After 10 alternate depositions of PVP and PAA, the $(HEP/CHI)_{10}$−$(PVP/PAA)_{10}$ multilayer film was constructed.

The cross-linking of the multilayer film was conducted by thermal treatments: 110 °C for different hours for formation of anhydride groups or 170 °C for 4 h for formation of ketone groups.[34]

For degradation experiments, the multilayer films were incubated in phosphate buffered saline (PBS) buffer at pH 7.4 at 37 °C for a predetermined time. The samples were then dried for bacterial adhesion and surface characterizations.

2.3. Antiadhesion of Bacteria Test (Water-Borne Assay). The multilayer film was immersed into a sterile plastic tube with 10 mL bacteria suspension (1.1×10^7 CFU/mL, in PBS buffer). The tube was shaken at 200 rpm at 37 °C for 5 min, 4 or 24 h. The sample was then washed gently three times with sterile PBS and immersed into glutaraldehyde solution (3 vol %, in PBS) at 4 °C for 4 h. After fixation and dehydration of the bacteria (25, 50, 70, 95, and 100 vol % ethanol for 10 min each), the sample was characterized by field-emission scanning electron microscope (FE-SEM, SiRion100).

2.4. Characterization Techniques. Thickness of the multilayer film was measured by spectroscopic ellipsometry (M-2000DI, Woollam). Continuous wavelength ranging from 124 to 1700 nm and angles of incidence (65° and 70°) were chosen for the ellipsometry measurements. The thickness that best fit the multilayer film can be automatically calculated from ellipsometry instrument.

Surface morphology was measured by atomic force microscope (AFM, SPA 400, Seiko). AFM was performed in the tapping mode under ambient conditions, equipped with a silicon cantilever (spring constant 40 N/m).

FE-SEM (SiRion100) was also used to measure thickness of the multilayer film. When the desired number of the film was deposited, after the drying process, the silicon wafers with the multilayer films were dried and snapped. The cross-sectional images of the multilayer films were obtained to measure the thickness.

Quartz crystal microbalance (QCM, QCM-E4, Q-Sense) measurements were carried out with an Au-coated resonator. The fundamental resonant frequency of the crystal was 5 MHz. The crystal was mounted in a fluid cell with one side exposed to the solution. A measurement of LbL deposition was initiated by switching the liquid exposed to the resonator. PEI (5 mg/mL) was allowed to contact with the resonator

Scheme 1. Schematic Representation of Construction, Cross-Linking, Degradation, and Antibacterial Properties of the $(HEP/CHI)_{10}$–$(PVP/PAA)_{10}$ Multilayer Film

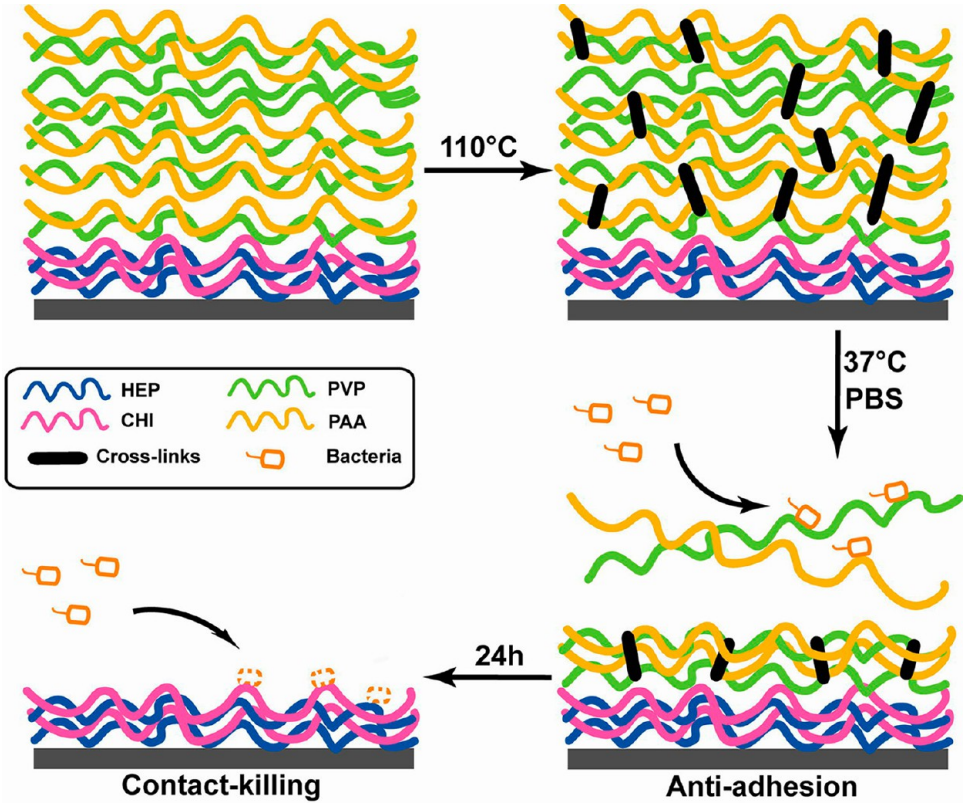

surface for 30 min for a precursor layer. Then, HEP and CHI solutions were alternately introduced for 10 min with buffer rinsing for 5 min in between. Both HEP and CHI were 1 mg/mL in HAc/NaAc buffer and injected into the fluid cell at a rate of 0.1 mL/min. After fabrication of the $(HEP/CHI)_{10}$ multilayer film, PVP and PAA solutions were alternately introduced at predetermined pH value for fabrication of the $(PVP/PAA)_{10}$ multilayer film.

Attenuated total reflectance (ATR) Fourier transform infrared (FTIR; E.S.P., MAGNA-IR560, Nicolet Instrument) measurements were carried out in the range of 3500 and 700 cm^{-1} at room temperature to analyze the multilayer films. Briefly, the $(HEP/CHI)_{10}$–$(PVP/PAA)_{10}$ multilayer film was fabricated onto PTFE substrates. The film was with or without thermal treatment at 110 °C for 16 h or 170 °C for 4 h. The ATR-FTIR spectra of the samples were obtained and analyzed.

A LIVE/DEAD BacLight bacterial viability kit (L-7012, Invitrogen) was used to determine bacterial cell viability. This test evaluate the structural integrity of bacterial membrane. After 24 h degradation, the multilayer films and control glass slides were incubated with *S. aureus* and stained according to the kit protocol. After careful wash, the samples were sealed with tin foil and observed by confocal laser scanning microscope (CLSM, ACAS, Ultima, Meridian Instruments).

All data were obtained from at least three independent experiments with five parallel samples and expressed as mean ± standard deviation (SD) and typical images.

3. RESULTS AND DISCUSSION

We aimed to design an enhanced antibacterial film through combining adhesion resistance and contact-killing strategies, as shown in Scheme 1. The multilayer film comprises two parts: (I) the top $(PVP/PAA)_{10}$ film is a top-down degradable part that can resist the adhesion of bacteria for 24 h, since the first 24 h after the implantation of biomedical devices is a critical period for bacterial adhesion, colonization, and formation of the biofilm; (II) the underlying $(HEP/CHI)_{10}$ film is a stable part for killing bacteria through contact type, endowing the surface with continual antibacterial properties.

3.1. Construction of the $(HEP/CHI)_{10}$–$(PVP/PAA)_{10}$ Multilayer Film. We first built the $(HEP/CHI)_{10}$ film on substrates. As shown in Figure 1, the thickness of the $(HEP/CHI)_n$ multilayer film increased linearly with 80.78 ± 4.31 nm for 10 bilayers number. In these depositions, the electrostatic adsorption is the main driving force.[18] PVP and PAA were then alternately deposited onto the $(HEP/CHI)_{10}$ film based on the hydrogen bond interaction, where PVP is the electron donor and PAA is the electron acceptor. It is reported that pH value

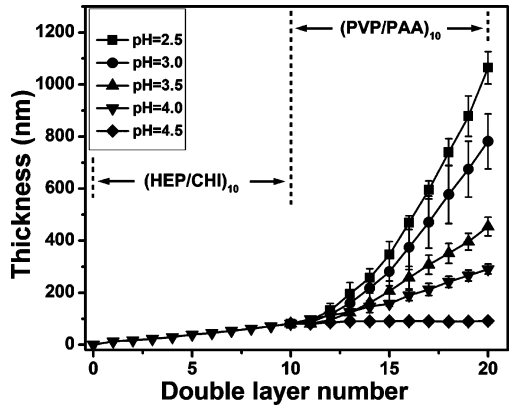

Figure 1. Ellipsometry measurement of the $(HEP/CHI)_{10}$–$(PVP/PAA)_{10}$ multilayer film. The $(HEP/CHI)_{10}$ film was constructed under HAc/NaAc buffer (0.1 M, pH = 4.0), and the $(PVP/PAA)_{10}$ films were deposited at different pH values.

dx.doi.org/10.1021/am4000547 | ACS Appl. Mater. Interfaces 2013, 5, 4136–4143

has a very important influence on the hydrogen bond interaction. We thereafter built a $(PVP/PAA)_n$ multilayer film at pH 2.5, 3.0, 3.5, 4.0, and 4.5 to determine the influence. All the films were constructed successfully, showing exponential growth, except for the film built under conditions of pH 4.5, as seen in Figure 1. However, growth of the multilayer film strongly depended on pH value. The lower the pH value of the solution, the faster the growth and the thicker the multilayer film obtained. This is a typical observation on the multilayer film based on hydrogen bonding. Similar growths were found by Ma et al.[35] in the build-up of (PVP/PAA) film and by Gu et al.[36] in the assembling of (PEO/PAA) film. Such a thick thickness is generally due to the "in and out" diffusion mechanism[37] and the increase of surface roughness with the number of deposited layers.[38] The $(HEP/CHI)_{10}$–$(PVP/PAA)_{10}$ multilayer film constructed at pH 3.0 was selected for the following experiments.

QCM with dissipation monitoring and AFM were used to follow the growth of the multilayer film as complementary characterizations. The change of QCM frequency confirmed successful construction of the $(HEP/CHI)_{10}$–$(PVP/PAA)_{10}$ multilayer film, showing a linear growth of the $(HEP/CHI)_{10}$ film and following an exponential growth of the $(PVP/PAA)_{10}$ film (Figure 2). The hydrogel nanofilms could be simulated

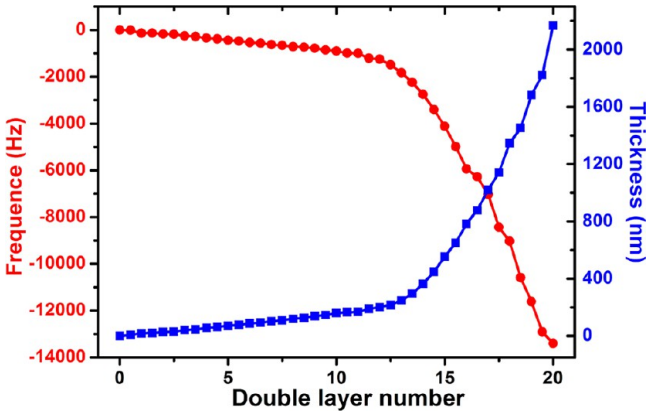

Figure 2. QCM measurement of construction of the $(HEP/CHI)_{10}$–$(PVP/PAA)_{10}$ multilayer film at pH 3.0: (●) frequency curve; (■) thickness curve of the multilayer film.

with the viscoelastic model by QCM-D analysis software to obtain the thickness.[39] The thicknesses of $(HEP/CHI)_{10}$ and $(PVP/PAA)_{10}$ film in the wet state reached ~159 and ~2008 nm, respectively, as seen in Figure 2. Correspondingly, based on ellipsometry measurement (Figure 1), the thicknesses of the multilayer films in the dry state were ~80 and ~701 nm. We then calculated that the swelling ratio of the $(HEP/CHI)_{10}$ and $(PVP/PAA)_{10}$ films were 198 and 286%, respectively. Such a high water incorporation is a typical phenomenon, particular in the multilayer films based on hydrogen bond interaction.[40]

The topographical features of the $(HEP/CHI)_{10}$–$(PVP/PAA)_n$ multilayer film were characterized by AFM. The micrographs of the multilayer films (n = 3, 6, 8, 10) were shown in Figure 3. The surfaces were relatively flat and smooth. Small particles and islets were found in the early stages of the $(PVP/PAA)_3$ multilayer film (Figure 3a). The surfaces became rougher with further deposition of the multilayer films. The root-mean-square (RMS) roughness (10 × 10 μm) was 4.5 ± 0.8, 5.6 ± 0.9, 8.4 ± 2.6, and 12.7 ± 3.2 nm for multilayer films with 3, 6, 8, and 10 bilayers, respectively, as determined by AFM. The AFM microimages not only indicated the successful assembly but also confirmed a relatively homogeneous surface of the $(HEP/CHI)_{10}$–$(PVP/PAA)_{10}$ multilayer films.

3.2. Controlled Degradation of the Top $(PVP/PAA)_{10}$ Multilayer Film. LbL assembly based on hydrogen bonds is of great interest as film disintegration happens upon external pH changes.[41] As in our (PVP/PAA) system, carboxylic acid groups on PAA, which are used to assemble the film as hydrogen bond acceptors, were deprotonated above a critical pH value. Thereby the hydrogen bond interactions between PAA and PVP were eliminated, leading to a very fast destruction of the film in a few minutes, as seen in Figure 4 (the multilayer film without thermal treatment). For the applications in the resistance of bacteria adhesion, controlling the destruction rate of the multilayer films is thus becoming a key point.

It was reported that PAA can be cross-linked by thermal treatment.[34] Generally, in low temperature (<150 °C), the major reaction during thermal cross-linking is the formation of anhydride groups. In the condition of higher temperatures (>150 °C), the anhydride concentration decreases and ester or ketone groups are formed.[42,43] It is well-known that anhydride group is easily hydrolyzed, while ester and ketone groups are stable. We thus think that the destruction of the (PVP/PAA) film could be regulated through thermal cross-linking at different temperatures. The $(HEP/CHI)_{10}$–$(PVP/PAA)_{10}$ multilayer films were cross-linked at 110 °C for different time. We also chose a higher temperature 170 °C for stronger cross-linking.[28] PBS buffer at 37 °C was selected to simulate a physiological condition. As shown in Figure 4, the degradation rate of the multilayer films was strongly depended on the time of thermal treatment. The longer the time of thermal cross-linking, the slower the degradation rate of the multilayer film. As expected, on the condition of thermal treatment at 170 °C, the multilayer films was stable with only about 5% thickness decreased in 24 h, which could be ascribed to the slow release of PVP molecules. This phenomenon suggested that the formation of anhydride group by 110 °C cross-linking is suitable for controlling degradation time of the multilayer films. One can observe that the multilayer films cross-linked at 110 °C for 16 h is the optimum for control of a complete degradation of the $(PVP/PAA)_{10}$ multilayer films in 24 h.

FTIR spectroscopy was used to determine the formation of anhydride and ketone groups during the thermal cross-linking. Figure 5 shows the spectra of the $(HEP/CHI)_{10}$–$(PVP/PAA)_{10}$ multilayer film with or without thermal treatments. The multilayer films without thermal treatment showed the absorption peaks close 3000 and 1709 cm^{-1} that indicated the carboxyl group in PAA, and absorption peaks at 1595 and 1450 cm^{-1} that indicated the ring vibration of pyridine of PVP.[44] In addition, the absorption peaks of 2530 and 1945 cm^{-1} that are assigned to O–H stretching vibration suggested the formation of stronger hydrogen bonds between PAA and PVP.[44] All these absorptions confirmed a successful construction of the $(HEP/CHI)_{10}$–$(PVP/PAA)_{10}$ multilayer film. After thermal treatment at 110 °C for 16 h, the disappearance of absorption peaks at 2530 and 1945 cm^{-1} and the appearance of absorption peaks at 1210 and 1020 cm^{-1}, which are assigned to strong C–O stretching vibration, indicated the formation of anhydride groups.[30,38,40] While in the case of thermal treatment at 170 °C for 4 h, the absorption peaks assigned to hydrogen and anhydride bonds were almost disappeared, and a weak

dx.doi.org/10.1021/am4000547 | ACS Appl. Mater. Interfaces 2013, 5, 4136–4143

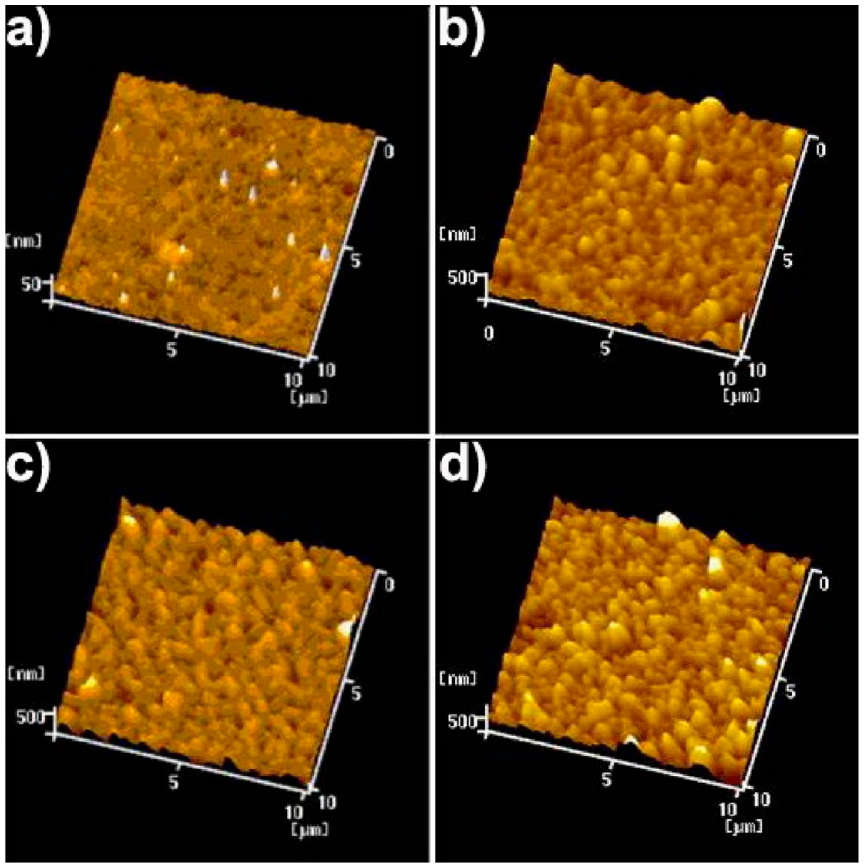

Figure 3. AFM measurement of topographical feature of the $(HEP/CHI)_{10}$–$(PVP/PAA)_n$ multilayer film at pH 3.0. Images showed different bilayer number with n = 3 (a), 6 (b), 8 (c), and 10 (d).

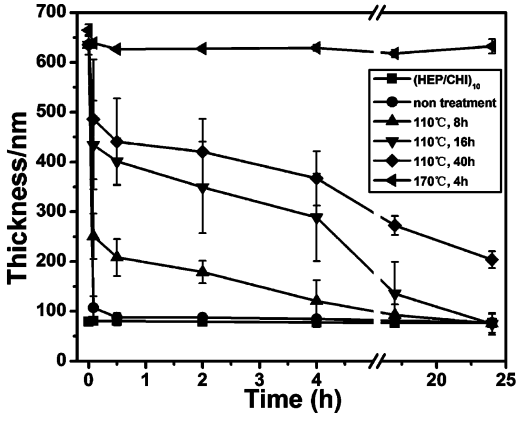

Figure 4. Thickness changes of the multilayer film in PBS buffer at 37 °C as measured by ellipsometry. The $(HEP/CHI)_{10}$–$(PVP/PAA)_{10}$ multilayer films were thermally treated at 170 °C for 4h (◀), 110 °C for 40 h (♦), 16 h (▼), and 8 h (▲), and nontreatment (●). The $(HEP/CHI)_{10}$ multilayer films without the top $(PVP/PAA)_{10}$ film was as control (■).

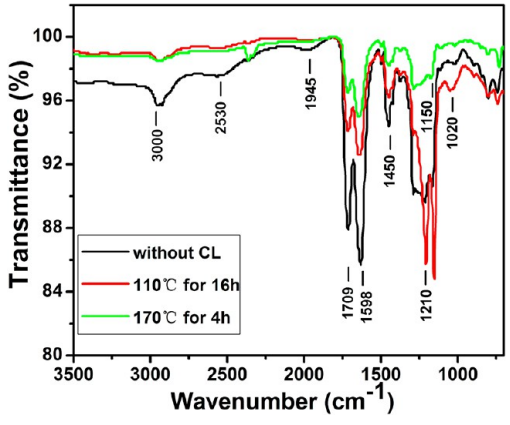

Figure 5. FTIR spectroscopy measurement of the $(HEP/CHI)_{10}$–$(PVP/PAA)_{10}$ multilayer film. The multilayer films were thermally treated at 110 °C for 16 h or 170 °C for 4 h.

absorption peak at 1150 cm^{-1} was appeared to indicate the formation of ketone groups.[42]

AFM was used to characterize the changes of topographical feature of the $(HEP/CHI)_{10}$–$(PVP/PAA)_{10}$ multilayer film (cross-linked at 110 °C for 16 h) during the degradation. As shown in Figure 6a–c, the surfaces became corrugated during the degradation. However, the multilayer films were still integral and relative smooth by and large. No breakdown or big holes were observed. The RMS roughness was increased from 12.7 ± 3.2 (before the degradation) to 17.2 ± 3.3 (0.5 h) and 21.2 ± 4.4 nm (4 h) and, then, decreased to 8.0 ± 1.1 nm, which could be ascribed to the exposure of the flat $(HEP/CHI)_{10}$ film after complete degradation of the $(PVP/PAA)_{10}$ film. These microimages suggested that the progressive degradation of the multilayer film occurred, rather than the bulk destruction. This is a key feature to ensure a continuous bacteria adhesion-resistance in the first critical 24 h after implantation.

SEM was then used to measure the thickness change of the multilayer film during the degradation. As can be seen in Figure

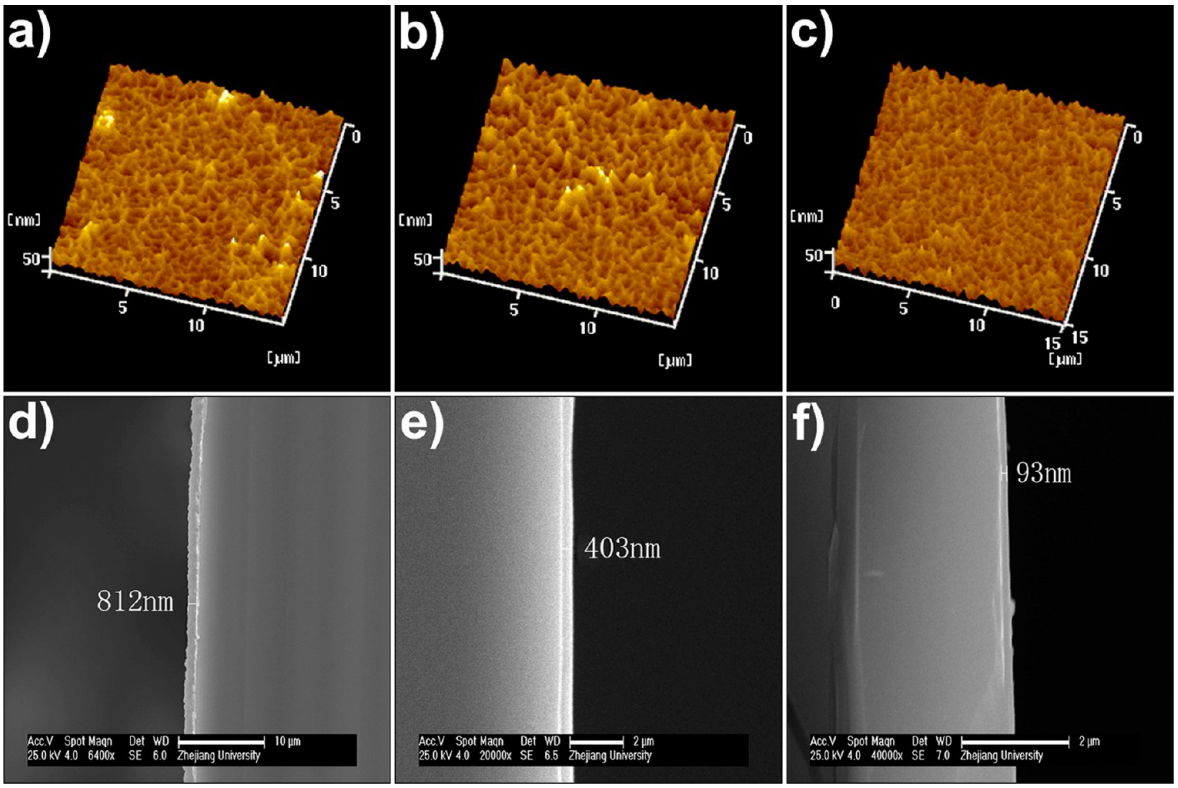

Figure 6. AFM measurement of topographical features of the $(HEP/CHI)_{10}$–$(PVP/PAA)_{10}$ multilayer films that have degraded in PBS buffer at 37 °C for 0.5 (a), 4 (b), and 24 h (c). The changes of thickness of the multilayer films were measured by SEM at time points 0 (d), 4 (e), and 24 h (f).

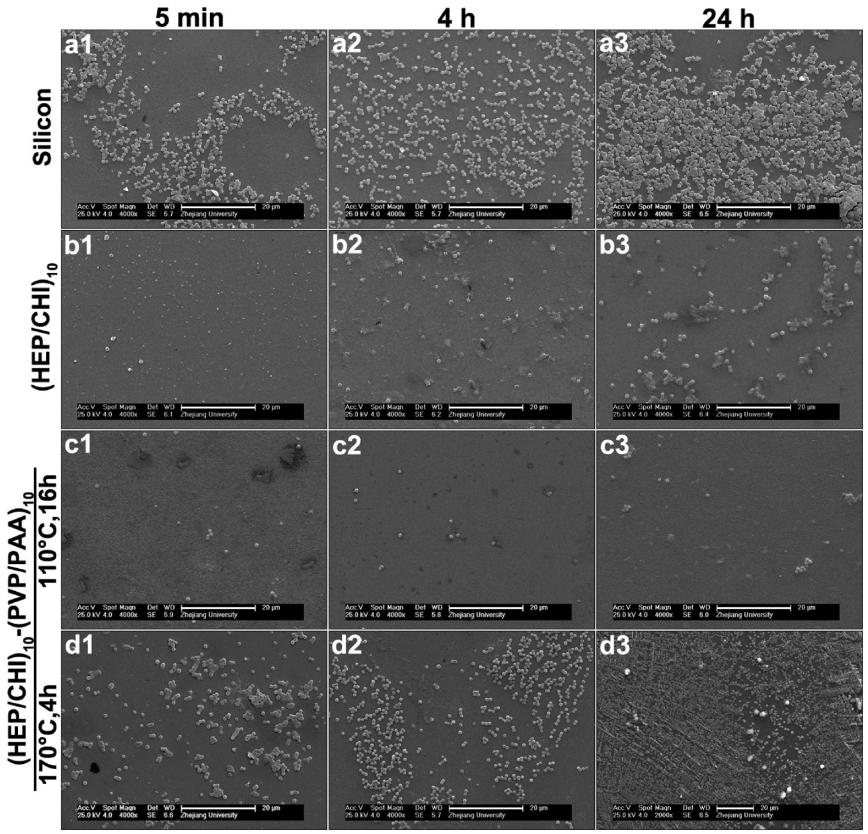

Figure 7. SEM images of water-borne assays of *S. aureus* adhesion on silicon wafer (a1–a3), the $(HEP/CHI)_{10}$ multilayer film (b1–b3), and the $(HEP/CHI)_{10}$–$(PVP/PAA)_{10}$ multilayer films cross-linked at 110 °C for 16 h (c1–c3) or at 170 °C for 4 h (d1–d3). Samples were measured after bacterial contacting for 5 min, 4 h, and 24 h. Scale bars are 20 μm.

dx.doi.org/10.1021/am4000547 | *ACS Appl. Mater. Interfaces* 2013, 5, 4136–4143

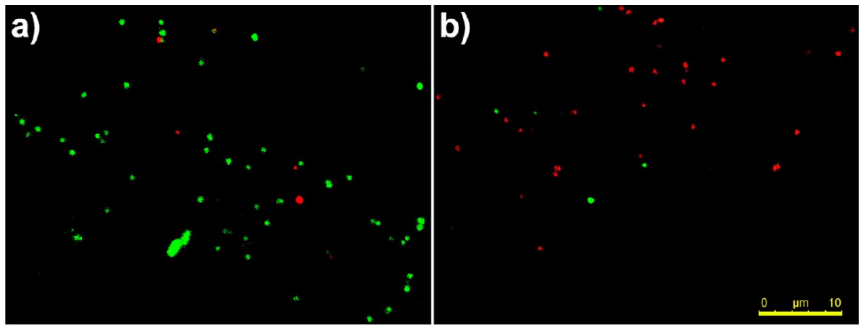

Figure 8. Fluorescent microscopy images of *S. aureus* adhesions on bare glass (a) and the $(HEP/CHI)_{10}$–$(PVP/PAA)_{10}$ multilayer film (b). The multilayer film was cross-linked at 110 °C for 16 h and then degraded in PBS buffer at 37 °C for 24 h. The green color indicates alive bacteria, and the red color indicates dead bacteria. Scale bar is 10 μm.

6d–f, before the degradation, the thickness of the multilayer film was 0.76 ± 0.24 μm. The thicknesses were then decreased to 0.38 ± 0.13 and 0.09 ± 0.01 μm at 4 and 24 h, respectively, during the degradation. There was almost 50% of the $(PVP/PAA)_{10}$ film degraded in the first 4 h. The degradation rate then became slower. After 24 h, according to the thickness, only the underlying $(HEP/CHI)_{10}$ film was left. These data are consistent with the data tested by spectroscopic ellipsometry (Figure 4), again confirming the continuous surface degradation.

3.3. Antibacterial Property of the $(HEP/CHI)_{10}$–$(PVP/PAA)_{10}$ Multilayer Film. The water-borne assay was employed to investigate the antiadhesion property of the multilayer film. *S. aureus* was selected as model bacteria, and a variety of samples, including silicon wafer, the $(HEP/CHI)_{10}$ multilayer film, and the $(HEP/CHI)_{10}$–$(PVP/PAA)_{10}$ multilayer films that thermal cross-linked at 110 °C for 16 h or 170 °C for 4 h, were chose for the bacteria adhesion assay. After contacting with bacteria suspension for 5 min, 4 h, and 24 h, one can observe that silicon wafer was very easy for bacteria adhesion even at initial 5 min. At 4 h, there were a larger number of bacteria adhering on the silicon wafer and the surface was almost covered by a layer of bacteria at 24 h, as seen in Figure 7a1–a3. In the case of the $(HEP/CHI)_{10}$ multilayer film, the number of adhered bacteria on the surface was significantly decreased at 5 min and 4 h (Figure 7b1 and b2), which could be due to hydrophilic HEP molecules.[18] A few bacteria were observed on the surface of the $(HEP/CHI)_{10}$ multilayer film after contacting with bacteria for 24 h (Figure 7b3). Actually, although HEP and CHI molecules can endow the films with the adhesion resistance and contact-killing of bacteria, the $(HEP/CHI)_{10}$ multilayer film can not resist bacteria for a long time, and bacteria cadavers that had been killed by CHI might be favorable for late bacterial adhesion. As we expected, the $(HEP/CHI)_{10}$–$(PVP/PAA)_{10}$ multilayer film, which was cross-linked at 110 °C for 16 h, showed an enhanced antiadhesion of bacteria, as shown in Figure 7c1–c3. There were only few bacteria adhering on the surface at 5 min, 4 h, and 24 h. While in the case of the nondegradable $(HEP/CHI)_{10}$–$(PVP/PAA)_{10}$ multilayer films that were cross-linked at 170 °C for 4 h, there were lots of adhered bacteria observed at 5 min and 4 h (Figure 7d1 and d2). After 24 h of contacting, the surface was almost completely covered by bacteria, as seen in Figure 7d3. The data thus suggest that continuous removal of the outmost surface is a key reason to inhibit bacteria adhesion. Such a dynamic surface could also be applicable in an in vivo environment to avoid the adsorption of protein or polysaccharide, which generally significantly impair the property of adhesion resistance.[45] We thus consider that the degradation gives the multilayer films advantages as compared with the superhydrophilic or superhydrophobic nonfouling surfaces.

After degradation of the $(PVP/PAA)_{10}$ multilayer film, the underlying $(HEP/CHI)_{10}$ multilayer film will be exposed to the external environment. It can thus provide contact-killing properties thereafter.[18] To confirm it, a LIVE/DEAD BacLight bacterial viability kit was used to stain the bacteria. Figure 8 shows bacteria on bare glass or the $(HEP/CHI)_{10}$–$(PVP/PAA)_{10}$ multilayer films. Because 24 h of degradation was allowed to occur before the staining process, the $(PVP/PAA)_{10}$ multilayer film was already completely removed, leading to the direct contact between bacteria and the $(HEP/CHI)_{10}$ multilayer films. One can observe that almost all of the adhered bacteria had been killed on the multilayer films, as seen in Figure 8b. As the control, the bacteria on bare glass were alive (Figure 8a). Such a subsequent contact-killing can thus endow the multilayer film with continual antibacterial properties.

4. CONCLUSIONS

The $(HEP/CHI)_{10}$–$(PVP/PAA)_{10}$ multilayer film based on electrostatic and hydrogen bond interactions was fabricated via LbL assembly. The QCM and ellipsometry results verified the progressive growth of the film. The AFM microimages demonstrated that surfaces of the multilayer films were relatively flat and RMS roughness increased slowly with the growth of the multilayer film. The $(PVP/PAA)_{10}$ multilayer film can be thermally cross-linked through formation of anhydride groups, and its cross-linking density can be modulated by time of thermal treatment. The $(PVP/PAA)_{10}$ multilayer films then showed a controlled top-down degradation, leading to an adhesion resistance of bacteria. In addition, after complete degradation of the top $(PVP/PAA)_{10}$ multilayer film, the underlying $(HEP/CHI)_{10}$ multilayer film subsequently provided the antibacterial property of contact-killing. Such an enhanced antibacterial film may have potential applications in the field of medical devices, particularly in implants.

AUTHOR INFORMATION

Corresponding Author

*Tel./Fax.: +86 571 87953729. E-mail address: renkf@zju.edu.cn (K.-f.R.); jijian@zju.edu.cn (J.J.).

Notes

The authors declare no competing financial interest.

■ ACKNOWLEDGMENTS

Financial support from the National Natural Science Foundation of China (50830106, 21174126, and 51103126), China National Funds for Distinguished Young Scientists (51025312), the National Basic Research Program of China (2011CB606203), Open Project of State Key Laboratory of Supramolecular Structure and Materials (SKLSSM201316), and Research Fund for the Doctoral Program of Higher Education of China (20110101110037 and 20110101120049) is gratefully acknowledged.

■ REFERENCES

(1) Kenawy, E.-R.; Worley, S. D.; Broughton, R. *Biomacromolecules* **2007**, *8*, 1359−1384.
(2) Neoh, K. G.; Hu, X. F.; Zheng, D.; Kang, E. T. *Biomaterials* **2012**, *33*, 2813−2822.
(3) Vasilev, K.; Cook, J.; Griesser, H. J. *Expert Rev. Med. Devic.* **2009**, *6*, 553−567.
(4) Costerton, J. W.; Stewart, P. S.; Greenberg, E. P. *Science* **1999**, *284*, 1318−1322.
(5) Lichter, J. A.; Van Vliet, K. J.; Rubner, M. F. *Macromolecules* **2009**, *42*, 8573−8586.
(6) Gon, S.; Kumar, K. N.; Nusslein, K.; Santore, M. M. *Macromolecules* **2012**, *45*, 8373−8381.
(7) Kingshott, P.; Wei, J.; Bagge-Ravn, D.; Gadegaard, N.; Gram, L. *Langmuir* **2003**, *19*, 6912−6921.
(8) Kaper, H. J.; Busscher, H. J.; Norde, W. *J. Biomat. Sci.—Polym. E.* **2003**, *14*, 313−324.
(9) Antonelli, P. J.; Sampson, E. M.; Ojano-Dirain, C. *Arch. Otolaryngol.−Head Neck Surg.* **2011**, *137*, 19−23.
(10) Tunney, M. M.; Gorman, S. P. *Biomaterials* **2002**, *23*, 4601−4608.
(11) Neoh, K. G.; Kang, E. T. *ACS Appl. Mater. Inter.* **2011**, *3*, 2808−2819.
(12) Genzer, J.; Efimenko, K. *Biofouling* **2006**, *22*, 339−360.
(13) Pernites, R. B.; Santos, C. M.; Maldonado, M.; Ponnapati, R. R.; Rodrigues, D. F.; Advincula, R. C. *Chem. Mater.* **2012**, *24*, 870−880.
(14) Hetrick, E. M.; Schoenfisch, M. H. *Chem. Soc. Rev.* **2006**, *35*, 780−789.
(15) Roy, D.; Knapp, J. S.; Guthrie, J. T.; Perrier, S. *Biomacromolecules* **2008**, *9*, 91−99.
(16) Yang, W. J.; Cai, T.; Neoh, K. G.; Kang, E. T.; Dickinson, G. H.; Teo, S. L. M.; Rittschof, D. *Langmuir* **2011**, *27*, 7065−7076.
(17) Sambhy, V.; Peterson, B. R.; Sen, A. *Langmuir* **2008**, *24*, 7549−7558.
(18) Fu, J. H.; Ji, J.; Yuan, W. Y.; Shen, J. C. *Biomaterials* **2005**, *26*, 6684−6692.
(19) Kenawy, E.-R.; Worley, S. D.; Broughton, R. *Biomacromolecules* **2007**, *8*, 1359−1384.
(20) Cheng, G.; Xue, H.; Zhang, Z.; Chen, S.; Jiang, S. *Angew. Chem., Int. Ed.* **2008**, *47*, 8831−8834.
(21) Shukla, A.; Fang, J. C.; Puranam, S.; Hammond, P. T. *J. Controlled Release* **2012**, *157*, 64−71.
(22) Rossi, S.; Azghani, A. O.; Omri, A. *J. Antimicrob. Chemoth.* **2004**, *54*, 1013−1018.
(23) Wang, B.-L.; Liu, X.-S.; Ji, Y.; Ren, K.-F.; Ji, J. *Carbohyd. Polym.* **2012**, *90*, 8−15.
(24) Fu, J.; Ji, J.; Fan, D.; Shen, J. *J. Biomed. Mater. Res. A* **2006**, *79A*, 665−674.
(25) Donlan, R. M.; Costerton, J. W. *Clin. Microbiol. Rev.* **2002**, *15*, 167−193.
(26) Mi, L.; Jiang, S. *Biomaterials* **2012**, *33*, 8928−8933.
(27) Poelstra, K. A.; Barekzi, N. A.; Rediske, A. M.; Felts, A. G.; Slunt, J. B.; Grainger, D. W. *J. Biomed. Mater. Res.* **2002**, *60*, 206−215.
(28) Yang, S. Y.; Rubner, M. F. *J. Am. Chem. Soc.* **2002**, *124*, 2100−2101.
(29) Wong, S. Y.; Moskowitz, J. S.; Veselinovic, J.; Rosario, R. A.; Timachova, K.; Blaisse, M. R.; Fuller, R. C.; Klibanov, A. M.; Hammond, P. T. *J. Am. Chem. Soc.* **2010**, *132*, 17840−17848.
(30) Higuchi, A.; Shirano, K.; Harashima, M.; Yoon, B. O.; Hara, M.; Hattori, M.; Imamura, K. *Biomaterials* **2002**, *23*, 2659−2666.
(31) Hayama, M.; Yamamoto, K.; Kohori, F.; Uesaka, T.; Ueno, Y.; Sugaya, H.; Itagaki, I.; Sakai, K. *Biomaterials* **2004**, *25*, 1019−1028.
(32) Devine, D. M.; Devery, S. M.; Lyons, J. G.; Geever, L. M.; Kennedy, J. E.; Higginbotham, C. L. *Int. J. Pharm.* **2006**, *326*, 50−59.
(33) Esman, N.; Peled, A.; Ben-Ishay, R.; Kapp-Barnea, Y.; Grigoriants, I.; Lellouche, J.-P. *J. Mater. Chem.* **2012**, *22*, 2208−2214.
(34) Maurer, J. J.; Eustace, D. J.; Ratcliffe, C. T. *Macromolecules* **1987**, *20*, 196−202.
(35) Ma, J.; Yang, S.; Li, Y.; Xu, X.; Xu, J. *Soft Matter* **2011**, *7*, 9435−9443.
(36) Gu, X.; Knorr, D. B., Jr.; Wang, G.; Overney, R. M. *Thin Solid Films* **2011**, *519*, 5955−5961.
(37) Shen, L.; Fu, J.; Fu, K.; Picart, C.; Ji, J. *Langmuir* **2010**, *26*, 16634−16637.
(38) Ji, J.; Fu, J. H.; Shen, J. C. *Adv. Mater.* **2006**, *18*, 1441−1444.
(39) Lin, Q.; Ding, X.; Qiu, F.; Song, X.; Fu, G.; Ji, J. *Biomaterials* **2010**, *31*, 4017−4025.
(40) Kharlampieva, E.; Sukhishvili, S. A. *Polym. Rev.* **2006**, *46*, 377−395.
(41) Yang, S.; Zhang, Y.; Zhang, X.; Xu, J. *Soft Matter* **2007**, *3*, 463−469.
(42) McGaugh, M. C.; Kottle, S. *J. Polym. Sci. B Polym. Lett.* **1967**, *5*, 817−820.
(43) Eisenber., A.; Yokoyama, T.; Sambalid., E. *J. Polym. Sci., Polym. Chem.* **1969**, *7*, 1717−1728.
(44) Wang, L. Y.; Fu, Y.; Wang, Z. Q.; Fan, Y. G.; Zhang, X. *Langmuir* **1999**, *15*, 1360−1363.
(45) Weir, E.; Lawlor, A.; Whelan, A.; Regan, F. *Analyst* **2008**, *133*, 835−845.